

Order in Phospholipid Langmuir-Blodgett Layers and the Effect of the Electrical Potential of the Substrate

Junlin Yang and J. Mieke Kleijn

Laboratory for Physical Chemistry and Colloid Science, Wageningen Agricultural University, 6703 HB Wageningen, The Netherlands

ABSTRACT The ordering in dipalmitoylphosphatidylcholine (DPPC) Langmuir-Blodgett monolayers and bilayers on a semiconducting indium tin oxide (ITO) surface has been investigated at the equilibrium potential of the interface and at various externally applied potentials. Second- and fourth-rank order parameters of a diphenylhexatriene (DPH) containing phospholipid probe were derived from total internal reflection fluorescence measurements, and orientation distributions were calculated using the maximum-entropy method. Generally, bimodal orientation distributions were obtained, suggesting that only part of the probes is aligned with the DPPC molecules. The effect of applied potentials is small for DPPC layers on unmodified (hydrophilic) ITO; with decreasing potential the ordering changes slightly to more random distributions, possibly because of the onset of hydrogen evolution at the substrate surface. For monolayers on hydrophobized ITO, where the phospholipids are initially with their tails directed toward the surface, the changes are more significant. At the highest positive potential applied, the derived order parameters indicate that nearly all probes are flat on the surface. This can be understood as a result of enhanced competition between headgroups and tails for access to the surface as it becomes more polarized. On unmodified ITO the electrochemistry of $\text{Fe}(\text{CN})_6^{3-/4-}$ and $\text{Ru}(\text{bipyridyl})_3^{2+/3+}$ is hardly hindered by the presence of DPPC monolayers or bilayers. On hydrophobized ITO a DPPC monolayer enhances the redox reactions.

INTRODUCTION

Phospholipid films on solid substrates are increasingly attracting attention as model systems for biological membranes, as well as for their application in electrochemical sensors and biosensors (Safinya, 1997). Recent advances in microelectronics, coupled with a sustained interest in ultra-thin phospholipid films, have stimulated many researchers to investigate the bilayer lipid membrane system as a basis for biomolecular devices (e.g., Kalb et al., 1990; Tien et al., 1993; Salamon et al., 1994; Siontorou et al., 1997).

A direct motivation for the present study comes from the work of Nelson, van Leeuwen, and Leermakers (Nelson and van Leeuwen, 1989a,b; Leermakers and Nelson, 1990; Nelson and Leermakers, 1990). They have shown that for a phospholipid monolayer adsorbed on a mercury electrode surface, the permeability for metal ions dramatically depends on the applied electrical potential as well as on the metal ion speciation. Using a theoretical model for the phospholipid monolayer, it was demonstrated that the potential-dependent behavior can be explained in terms of structural variations (phase transitions) of the phospholipid monolayers. These phase transitions are not of physiological importance, but their occurrence might be exploited to detect compounds in very low concentrations: from both experiments and theoretical calculations, it has been found that details of the transitions are very sensitive to additives

in the system. The calculations also showed that the segment density profile for a lipid monolayer on a solid substrate resembles half the profile for a lamellar bilayer membrane, suggesting that such monolayers are suitable model systems for the study of permeation properties of biomembranes.

With total internal reflection fluorescence (TIRF) it is possible to determine the second- and fourth-rank order parameters ($\langle P_2 \rangle$ and $\langle P_4 \rangle$) of the orientation distribution of fluorophores in an adsorption layer on an optically transparent substrate (Bos and Kleijn, 1995a). To apply this method to phospholipid layers, it is necessary to build in fluorescent probes. Recently, we presented the first results of TIRF orientation measurements on dipalmitoylphosphatidylcholine (DPPC) monolayers transferred on quartz by the Langmuir-Blodgett (LB) technique (Zhai and Kleijn, 1997a). By using optically transparent and conductive films deposited on quartz slides as the substrates, TIRF can be combined with electrochemical techniques. This allows, for example, determination of the order in the phospholipid layers as a function of an externally applied interfacial potential.

In this paper we report on TIRF orientation measurements on DPPC monolayers and bilayers transferred from the liquid-condensed state onto indium tin oxide (ITO) films on quartz plates. 2-(3-(Diphenyl-hexatrienyl)propanoyl)-1-hexadecanoyl-sn-glycero-3-phosphocholine (DPH₆PC) is used as a fluorescent probe. ITO is a semiconductor with a relatively high conductivity. The ITO surface is hydrophilic, which implies that phospholipids transferred to it by the Langmuir-Blodgett technique are with their headgroups on the surface. To enable a better comparison with results obtained for phospholipid monolayers on mercury (a hydrophobic surface), we also prepared monolayers on hydropho-

Received for publication 18 February 1998 and in final form 1 September 1998.

Address reprint requests to Dr. J. Mieke Kleijn, Laboratory for Physical Chemistry and Colloid Science, Wageningen Agricultural University, Dreijenplein 6, 6703 HB Wageningen, The Netherlands. Tel.: 31-317-482145/482178; Fax: 31-317-483777; E-mail: mieke@fenk.wau.nl.

© 1999 by the Biophysical Society

0006-3495/99/01/323/10 \$2.00

bized ITO, in which the lipid chains are directed to the substrate surface. Apart from orientation measurements as a function of applied potential, we investigated the effect of the presence of DPPC monolayers and bilayers at unmodified and hydrophobized ITO surfaces on the electrochemistry of two redox couples, hexacyanoferrate ($\text{Fe}(\text{CN})_6^{4-/3-}$) and ruthenium trisbipyridyl ($\text{Ru}(\text{bipyridyl})_3^{2+/3+}$).

MATERIALS AND METHODS

DPPC (1,2-dihexadecanoyl-sn-glycerol-3-phosphocholine) was obtained from Fluka. 2-(3-(Diphenylhexatrienyl)-1-hexadecanoyl-sn-glycero-3-phosphocholine (DPH₆PC) was purchased from Molecular Probes Europe BV (Leiden, the Netherlands). $\text{K}_3\text{Fe}(\text{CN})_6$ and $\text{Ru}(\text{bipyridyl})_3\text{Cl}_2$ were obtained from Merck and Fluka, respectively. All chemicals were used without further purification.

Indium tin oxide (ITO) films were dc sputtered onto quartz slides (Suprasil 2; Heraeus Quartz Glass GmbH, Hanau, Germany) by Philips Flat Panel Display Co. (Eindhoven, The Netherlands). These ITO films contain 10% Sn, and their thickness is 115 nm as measured by ellipsometry. The point of zero charge of the ITO films in contact with aqueous solutions is approximately at pH 3 (Bos et al., 1994).

Langmuir-Blodgett film transfer

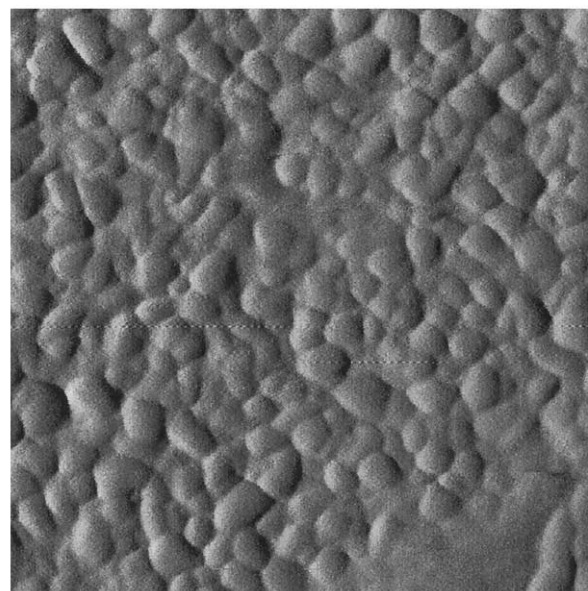
A home-made Langmuir trough (area 600 cm²), equipped with a microbalance for surface pressure measurement by the Wilhelmy-plate method, was used for monolayer transfer. A mixture of DPPC and DPH₆PC (molar ratio 20:1) dissolved in chloroform was spread on a subphase of pure water (resistance 18.3 M Ω /cm). After solvent evaporation the monolayer was compressed to a prespecified surface pressure. Subsequently, the monolayer was allowed to relax for 1 h.

Transfer to an ITO/quartz plate was carried out by lifting the substrate vertically out of the subphase at a speed of 0.8 mm²/s. Before transfer the ITO/quartz plates were cleaned by overnight immersion in a base alcoholic solution, followed by UV-ozone treatment, and then rinsed with water. DPPC/DPH₆PC monolayers were transferred at a surface pressure of 30 mN/m, i.e., from the liquid-condensed phase at the air/water interface (Mitchell and Dluhy, 1988). All film transfers were performed at a temperature of $20 \pm 1^\circ\text{C}$, and in all cases the transfer ratios were larger than 95%. Fluorescence measurements confirmed incorporation of the probe molecules into the supported monolayers.

DPPC/DPH₆PC bilayers were prepared following the method described by Tamm and McConnell (1985). In short, the first layer was transferred to the substrate as described above. For the second layer, the ITO/quartz plate coated with a monolayer was pushed through the air/water interface horizontally at slow speed. This results in a decrease in the surface pressure, and recompression yielded an area decrease of the monolayer on the air/water interface corresponding to ~ 1.2 times the area of one side of the substrate. To check whether a bilayer is actually formed on the ITO/quartz plate, the thickness of the transferred film was measured by ellipsometry. The thickness measured for a bilayer is ~ 8.5 nm, whereas for a monolayer this was found to be ~ 3.6 nm. The influence of a DPPC monolayer and a DPPC bilayer on the surface topography of the substrate was examined with an atomic force microscope (NanoScope III; Digital Instruments, Santa Barbara, CA) (see Fig. 1). The mean roughness of the bare ITO surface was found to be ~ 2.0 nm over a scan area of 1 μm . For the phospholipid covered ITO surfaces this is lower: 1.2 nm for a monolayer and 0.6 nm for a bilayer. A decrease in surface corrugation caused by LB film transfer is a well-known phenomenon (see, e.g., Mikrut et al., 1993; Gu et al., 1995; Zhai and Kleijn, 1997b). AFM images of the monolayers and bilayers did not reveal (pin)holes in these layers.

ITO surfaces were rendered hydrophobic by immersion in a solution of 0.5% dichlorodimethylsilane in trichloroethane for 30 min. Afterward, the

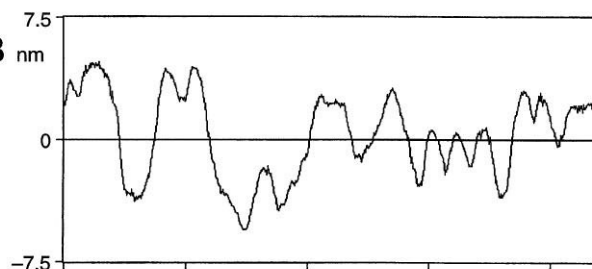
A



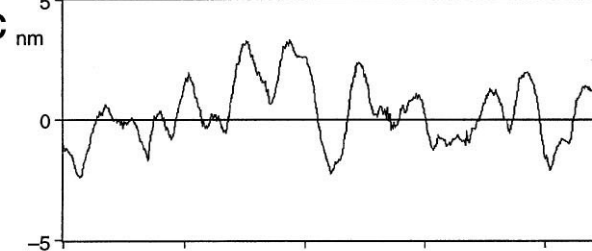
0

1.00 μm

B
nm



C
nm



D
nm

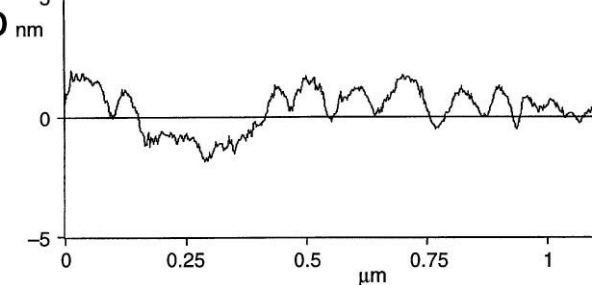


FIGURE 1 (a) AFM image of the bare ITO surface. (b) Cross section of the bare ITO surface. (c) Cross section of ITO covered with a DPPC/DPH₆PC monolayer. (d) Cross section of ITO covered with a DPPC/DPH₆PC bilayer.

plates were rinsed with ethanol and water, in that order. The result is a methylated ITO surface (ITO-CH₃). Transfer of DPPC/DPH₆PC monolayers to hydrophobized ITO surfaces was done in the same way as for

unmodified ITO, except for that the transfer was carried out by moving the substrate vertically down into the subphase. In Fig. 2 the structures of the various types of phospholipid layers studied here are schematically given.

TIRF orientation measurements

The TIRF set-up and the way of data acquisition and data handling have been described in detail before (Bos and Kleijn, 1995b; Zhai and Kleijn, 1997a). An ITO/quartz plate was mounted on the TIRF cell, and the quartz side of the plate was optically coupled to a quartz prism with immersion oil. Subsequently, the cell was filled with water or an aqueous electrolyte solution. The ITO side of the plate (with or without phospholipid layer) was in contact with the solution in the cell. A pulsed nitrogen laser (model VSL-337ND; Laser Science, Cambridge, MA) with an emission wavelength of 337 nm was utilized for excitation. After passing a polarization rotator (Berek polarization compensator, model 5540; New Focus, Mountain View, CA), the laser beam entered the prism, was transmitted through the quartz slide, and was totally reflected at the ITO/solution interface, resulting in an evanescent field at the solution side of the interface and excitation of the DPH probes (if present). The excitation spot at the solid/liquid interface was $\sim 1 \text{ mm}^2$.

Detection of the fluorescence was performed at a wavelength of 478 nm. At different locations on a supported phospholipid layer both the parallel and perpendicular polarized components of the fluorescence were measured repeatedly in series of 100 laser pulses. This was done for polarization angles Ψ of the incident laser beam of 0° and 90° with respect to the plane of incidence. This procedure yields four fluorescence components for each location on the LB film: $F_{\parallel}(0^\circ)$, $F_{\perp}(0^\circ)$, $F_{\parallel}(90^\circ)$, and $F_{\perp}(90^\circ)$. Before each series of measurements on a supported phospholipid layer, a controlled background experiment on a bare ITO/quartz slide was carried out to correct for contributions to the fluorescence by parts of the TIRF cell excited by scattered radiation. All TIRF measurements were performed at room temperature.

The theoretical background of the orientation measurements has been discussed before in general terms (Bos and Kleijn, 1995a) and specifically for DPH (diphenylhexatriene)-based probes in phospholipid films (Zhai and Kleijn, 1997a). It has been shown that the intensity of the fluorescence signal F is a linear function of $\cos^2\Psi$:

$$F_{\parallel}(\Psi) = C(A_{\parallel} + B_{\parallel}\cos^2\Psi) \quad (1a)$$

$$F_{\perp}(\Psi) = C(A_{\perp} + B_{\perp}\cos^2\Psi) \quad (1b)$$

The parameters A_{\parallel} , B_{\parallel} , A_{\perp} , and B_{\perp} depend on the orientation distribution of the fluorescent probes, the angle β between the absorption and emission dipole moments of the probes, and the components of the evanescent field, ϵ_x , ϵ_y , and ϵ_z . Elaborate expressions for $F_{\parallel}(\Psi)$ and $F_{\perp}(\Psi)$ and the definitions of ϵ_x , ϵ_y , and ϵ_z are given in the previous paper (Zhai and Kleijn, 1997a). The proportionality constant C depends on variables such as the surface concentration of fluorescent probes, the intensity of the incident laser beam, the fluorescence quantum yield, and properties of the detection system. From Eq. 1 it follows that measuring the four fluorescence components $F_{\parallel}(0^\circ)$, $F_{\perp}(0^\circ)$, $F_{\parallel}(90^\circ)$, and $F_{\perp}(90^\circ)$ suffices to disclose all available information concerning the orientation distribution of the probes as reflected in the fluorescence response of the system. This information

involves the second- and fourth-rank order parameters of the orientation distribution of the fluorophores, $\langle P_2 \rangle$ and $\langle P_4 \rangle$, which are defined as

$$\langle P_2 \rangle = \frac{1}{2} (3\langle \cos^2\theta \rangle - 1) \quad (2a)$$

$$\langle P_4 \rangle = \frac{1}{8} (35\langle \cos^4\theta \rangle - 30\langle \cos^2\theta \rangle + 3) \quad (2b)$$

in which θ represents the angle between the direction of the absorption dipole moment of the DPH group and the normal of the interface. The brackets $\langle \rangle$ denote an average over all abundant orientations.

For analysis of the data in terms of order parameters of the DPH probes, for the components of the evanescent field, ϵ_x , ϵ_y , and ϵ_z , values of 0.3540, 0.7292, and 0.9842 were used, respectively. These values were calculated using Abeles' method for reflectivities (Hansen, 1968) with refractive indices of 1.479 for quartz in the UV region, 1.90 for the ITO film, and 1.333 for the aqueous solution, the thickness of the ITO film (115 nm), and an angle of incidence of the laser beam of 75° . To obtain $\langle P_2 \rangle$ and $\langle P_4 \rangle$ from a set of the four fluorescence components, a least-squares numerical fit was performed. In this way we derived the $(C, \langle P_2 \rangle, \langle P_4 \rangle)$ parameters for different values of β . Subsequently, for β the value was taken that yielded the best fit, with $\langle P_2 \rangle$ and $\langle P_4 \rangle$ located within their physical boundaries, which follow from their definition given in Eq. 2.

Potential-dependent orientation measurements and voltammetry

Variation of the electrical potential of the substrate and voltammetric experiments were carried out in the TIRF cell at room temperature. The ITO/quartz plate in this cell was the working electrode. A Pt wire was used as a counterelectrode, and the reference electrode was an Ag/AgCl/saturated KCl electrode (+0.222 V versus NHE). Cyclic voltammetric curves were measured at various scan rates in 0.1 M KNO_3 solution. $\text{Fe}(\text{CN})_6^{3-}$ or $\text{Ru}(\text{bipyridyl})_3^{2+}$ at a concentration of $1.0 \times 10^{-3} \text{ M}$ was used as the electroactive species. Before each experiment the solutions were flushed with nitrogen gas for at least half an hour. Potentials were applied from a Princeton Applied Research Polarographic analyzer (model 174A).

RESULTS AND DISCUSSION

Orientalional order in DPPC monolayers and bilayers on ITO

For each type of supported phospholipid layer studied here, a number of orientation measurements have been performed on various ITO/quartz plates and at different locations on these plates. It was found that on a particular substrate the total fluorescence intensity is practically the same at every position. As expected, the intensity of fluorescence from the bilayers is substantially higher than that from the monolayers (typically 1.8 times as high, sometimes twice as high). The results in terms of order parameters are depicted in Fig. 3. All of the experimental data obtained in the present study yielded $\langle P_2 \rangle$ and $\langle P_4 \rangle$ combinations within their physical boundaries for values of β (the angle between absorption and emission dipole moment) around 32° . The spread in the β values over all sets of data collected from one type of lipid layer was found to be very small ($<1^\circ$). Average (overall) order parameters for each type of phospholipid layer are listed in Table 1. These average values for $\langle P_2 \rangle$ and $\langle P_4 \rangle$ were obtained by fitting all data sets, i.e., all measured

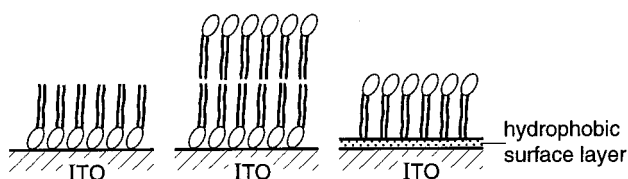


FIGURE 2 Schematic representation of the structures of the supported phospholipid layers studied here.

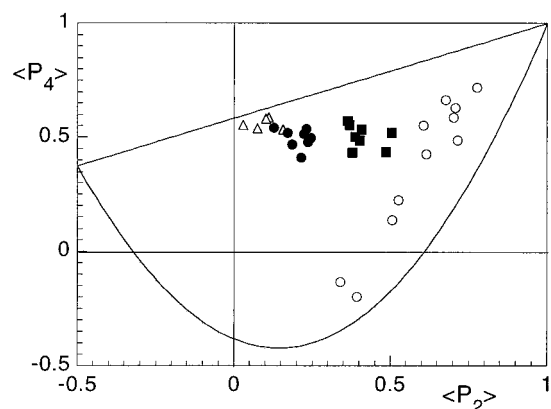


FIGURE 3 Combinations of order parameters $\langle P_2 \rangle$ and $\langle P_4 \rangle$ obtained for DPPC/DPHPC monolayers (●) and bilayers (■) on hydrophilic ITO, and for monolayers on hydrophobized ITO (△). Earlier results obtained for similar monolayers on quartz are also depicted (○) (Zhai and Kleijn, 1997a). The solid curves indicate the physical boundaries for $\langle P_2 \rangle$ and $\langle P_4 \rangle$.

combinations of the four fluorescence components, for a particular type of lipid layer in one time.

The earlier obtained results for DPPC/DPHPC monolayers on quartz transferred at 30 mN/m are given in Fig. 3 and Table 1 (Zhai and Kleijn, 1997a). These monolayers were prepared under exactly the same conditions and have the same composition as the monolayers on the unmodified ITO/quartz plates in this study. Furthermore, in Table 1 results are given for DPPC/DPHPC monolayers on quartz transferred at a low surface pressure of 6.5 mN/m and for DPPC/TMA-DPH on quartz transferred at 30 mN/m. (TMA-DPH represents the fluorescent probe molecule 1-(4-trimethylammoniumphenyl)-6-phenyl-1,3,5-hexatriene.)

From the second- and fourth-rank order parameters and using the so-called maximum-entropy method, an approximation of the angular distribution function $N(\theta)$ and the corresponding number density functions $N(\theta)\sin\theta$ for the various types of layers can be obtained (Bos and Kleijn, 1995a; Zhai and Kleijn, 1997a). In Fig. 4 orientation distributions are given that have been calculated from the average (overall) order parameters listed in Table 1 according to the maximum-entropy method. Bimodal orientation distributions are obtained, not only for these average $(\langle P_2 \rangle, \langle P_4 \rangle)$ combinations, but for all combinations of order parameters

TABLE 1 Average order parameters and angle between absorption and emission dipole moments of the DPH group for various supported phospholipid layers

| Layer type | $\langle P_2 \rangle$ | $\langle P_4 \rangle$ | β |
|---|-----------------------|-----------------------|---------|
| DPPC/DPHPC monolayer on ITO | 0.21 | 0.50 | 32° |
| DPPC/DPHPC bilayer on ITO | 0.43 | 0.63 | 33° |
| DPPC/DPHPC monolayer on hydrophobized ITO | 0.11 | 0.59 | 32° |
| DPPC/DPHPC monolayer on quartz* | 0.60 | 0.37 | 0° |
| DPPC/DPHPC monolayer on quartz, 6.5 mN/m* | 0.09 | 0.25 | 36° |
| DPPC/TMA-DPH monolayer on quartz* | 0.27 | 0.63 | 32° |

All layers were transferred at 30 mN/m unless indicated otherwise.

*Results from Zhai and Kleijn (1997a).

for DPPC/DPHPC layers on ITO as shown in Fig. 3. In all cases a maximum in the number density function is found at $\theta = 90^\circ$, suggesting that a (substantial) part of the probe molecules lies more or less parallel to the substrate surface. The position of the other maximum varies between 7° and 11° for monolayers on unmodified ITO, 5° and 8° for monolayers on hydrophobized ITO, and 8° and 12° for bilayers on unmodified ITO. This maximum may be interpreted as reflecting the part of the fluorescent probe molecules aligned with their DPH-containing tail parallel to the acyl chains of the DPPC molecules.

It seems energetically unfavorable to have a significant part of the fluorescent phospholipids in a parallel orientation. If there is indeed such a fraction, this implies that there are strong (favorable) interactions between the DPH-containing tail of the probe molecule and the substrate surface. Then the parallel oriented probes are located between the ITO surface and the headgroups of the DPPC molecules. This seems to be corroborated by the fraction of the DPHPC molecules oriented parallel to the substrate being smaller for a bilayer than for a monolayer on ITO. (This is a significant feature, observed for all orientation distributions corresponding to the $(\langle P_2 \rangle, \langle P_4 \rangle)$ combinations con-

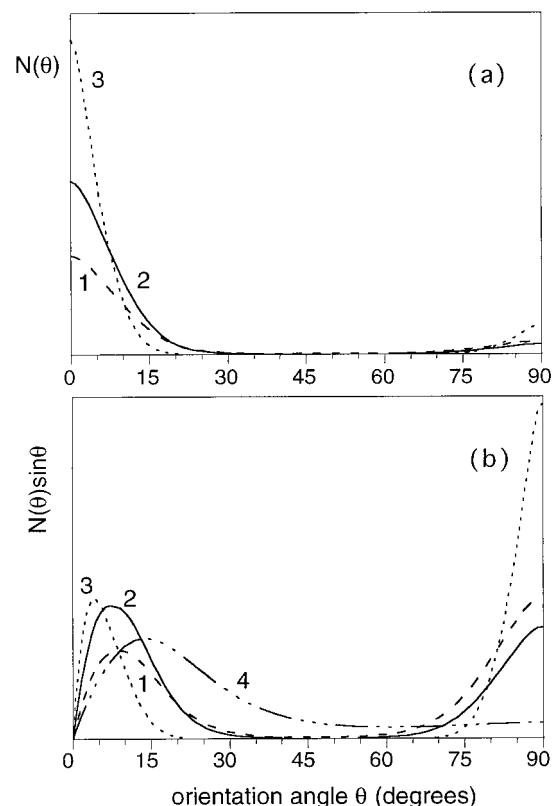


FIGURE 4 (a) Angular orientation distributions for DPPC/DPHPC layers transferred at 30 mN/m, as calculated from the average order parameters in Table 1 according to the maximum-entropy method. (1) Monolayers on hydrophilic ITO. (2) Bilayers on hydrophilic ITO. (3) Monolayers on hydrophobized ITO. (b) Corresponding number density functions. Also shown is the number density function for DPPC/DPHPC monolayers on quartz (4) (Zhai and Kleijn, 1997a).

cerned in Fig. 3.) After all, it is very unlikely that probe molecules from the second layer will move to the ITO surface. (In contrast to the free probe molecule DPH, DPHpPC does not tend to locate in the center of and parallel to lipid bilayers (Lentz, 1989)). For hydrophobized ITO the fraction parallel oriented probes is larger than for unmodified ITO. Moreover, the maxima in the number density functions for the monolayers on hydrophobized ITO are significantly sharper, which may arise from the fact that in this monolayer the phospholipid tails are confined in their freedom of movement.

With respect to the above interpretation of the measured data, we have to point to some (possibly serious) limitations. In the first place, it should be realized that it is not possible to retrieve the exact orientation distribution in all of its details from two order parameters only. Application of the maximum-entropy method merely results in the smoothest and broadest distribution consistent with the limited data at our disposal and maximally noncommittal with respect to unavailable data (Bevensee, 1983). Therefore, some reserves are appropriate regarding the conversion of the derived order parameters into orientation distributions. What is definitely clear, however, is that model orientation distributions with only one maximum (e.g., the Gaussian distribution) are not consistent with the $\langle P_2 \rangle$, $\langle P_4 \rangle$ combinations derived here.

Second, the analysis of the fluorescence data is based on a theoretical model (described in detail in the previous paper by Zhai and Kleijn, 1997a) in which DPH is considered as a cylindrically symmetrical moiety with its absorption dipole moment parallel to the long molecular axis (Lentz, 1989). This description of the probe gives satisfactory results for organized phospholipid systems in solution, as has been shown by several fluorescence depolarization studies (Kooyman et al., 1983; Deinum et al., 1988; Muller et al., 1994a,b; Florine-Casteel, 1990), as well as for TIRF orientation measurements performed on DPPC/DPHpPC monolayers on quartz (Zhai and Kleijn, 1997a). It may be that complicated interactions among conjugated DPH and the ITO substrate result in violations of the cylindrical symmetry and probe geometry assumptions. Such interfering interactions may be especially expected for probes flat on the surface, and therefore the data analysis may be less accurate, as the fraction of parallel oriented DPHpPC molecules is larger. In any event, the interaction between DPH and a solid substrate (ITO as well as quartz) seems to result in larger values for the angle between absorption and emission dipole moment of the probes; we return to this issue later in this discussion.

Other assumptions in the model underlying the data analysis are that the orientation of the probes does not change on the time scale of fluorescence and that the angle β between absorption and emission dipole moment is the same for all probe molecules in a particular type of lipid layer. In fact, the derived value for β is a kind of time and ensemble average (Zhai and Kleijn, 1997a) and rotations with time scales comparable to or shorter than the average fluores-

cence lifetime of DPH may contribute to this value. However, for the TIRF orientation measurements the only mode that gives rise to fluorescence depolarization is rotational diffusion along directions perpendicular to the long symmetry axis of the DPH moiety, for lipid bilayers usually described as wobbling motion (Cheng, 1989), and internal motions of the DPH moiety within the probe lipids. Rapid rotations along the long axis of the probe molecules do not affect the TIRF orientation measurements, provided that the assumption of the alignment of the absorption dipole moment along the DPH-containing tail of the probe molecules is justified. For these rapid rotations correlation times in the same range as the fluorescence lifetimes have been reported for DPHpPC in gel-phase lipid bilayers, i.e., between 1 and 8 ns (Mulders et al., 1986; Cheng, 1989; Muller et al., 1994a,b; Bernsdorff et al., 1995; Parente and Lentz, 1985; Van Ginkel et al., 1986; Cheng, 1989; Lentz, 1989; Bernsdorff et al., 1995). On the other hand, wobbling motions are fairly restricted in the gel phase, with maximum deviations of 10–20° from the mean orientation angle (Parente and Lentz, 1985; Lentz, 1989; Florine-Casteel, 1990). It is to be expected that for phospholipid monolayers and bilayers on solid substrates, rotational diffusion is even more restricted, although we cannot entirely exclude some “dynamic” contribution to the derived values of β and the order parameters.

In this study we have found β values around 32° for all DPPC/DPHpPC monolayers and bilayers on ITO, which is in reasonable agreement with literature data. For DPH-based probes, values for β ranging from 0° to 35° have been reported (Kooyman et al., 1983; Van Ginkel et al., 1986; Deinum et al., 1988; Cheng, 1989; Muller et al., 1994a,b, 1996). It should be noted, however, that these are all for lamellar phospholipid systems in solution and not for phospholipid mono- or bilayers on solid substrates. It has been established by several authors that for DPH probe molecules the angle β between absorption and emission dipole moments depends on the molecular environment (Kooyman et al., 1983; Van Ginkel et al., 1986; Van Langen et al., 1987; Deinum et al., 1988). If the DPH molecules can be divided into two populations (molecules that are lying flat, probably between substrate surface and phospholipid headgroups, and molecules that are aligned with the DPPC molecules), there may be also a bimodal distribution in β . Provided that β is not directly correlated with the molecular tilt angle, this has no consequences for our analysis. The limited number of parameters that can be extracted from the experimental data does not allow for any conclusion with respect to the distribution in β .

The combinations of order parameters obtained for the monolayers on unmodified ITO differ substantially from the earlier obtained results for similar monolayers on quartz (Table 1, Figs. 3 and 4). For quartz as the substrate, order parameters corresponding to unimodal orientation distributions have been derived. As discussed before, an explanation for the difference in orientation distributions may be provided by specific interactions between the DPH-containing tail of the probe molecule and the substrate surface; if

so, these must be significantly stronger for ITO than for quartz. Another aspect in which the quartz and ITO surface differ is their surface roughness: quartz is less corrugated (mean roughness ~ 0.5 nm; Zhai and Kleijn, 1997b) than ITO (~ 2 nm). However, a larger surface roughness would merely result in a broader orientation distribution (i.e., not only a lower value for $\langle P_2 \rangle$, but also for $\langle P_4 \rangle$). Furthermore, when looking at the cross section of the ITO surface (Fig. 1 *b*), it can be seen that the slopes of the irregularities are relatively small (less than $\sim 10^\circ$; note the scale differences for the horizontal and the vertical axes) and are not expected to have a large influence on the orientation distribution in the phospholipid layer.

Fig. 3 also shows that the scatter in the obtained combinations of order parameters is less for the monolayers on ITO than for those on quartz. This scatter reflects, besides nonsystematic experimental errors and uncertainties in the analysis in terms of order parameters (which are in the same order for ITO and quartz), intrinsic differences in the original fluorescence data measured at different locations of the LB films. Apparently, local variations in the ordering in the monolayers on ITO are smaller than for those on quartz.

For DPPC/DPH₂PC monolayers on quartz transferred at 30 mN/m it has been found that the absorption and emission dipole moments of the probe are practically colinear ($\beta \approx 0$; Table 1). Here, for similar monolayers on ITO, a value for β of $\sim 32^\circ$ is derived. This is the same as the value found for DPPC/TMA-DPH monolayers on quartz transferred at 30 mN/m. The orientation distribution of TMA-DPH on quartz calculated from the obtained order parameters is also bimodal and looks much the same as the one for the DPPC/DPH₂PC monolayers on ITO (see Zhai and Kleijn, 1997a). Bimodal distributions for TMA-DPH have also been reported for TMA-DPH in lipid bilayer systems, from a fluorescence depolarization study on DPPC vesicles (Florine-Casteel, 1990) and from neutron scattering experiments on DPPC multilayers on glass (Pebay-Peyroula et al., 1994). As mentioned before, for DPH-containing probes the angle between absorption and emission dipole moments depends on their molecular environment. Apparently, interaction with a solid substrate (ITO or quartz) induces a change in β to larger values. For DPPC/DPH₂PC monolayers transferred to quartz at a low surface pressure of 6.5 mN/m, most of the probes are oriented parallel to the substrate surface, and an even larger value for β has been found (36°). For these loosely packed monolayers, however, the interaction between DPH and the aqueous solution may also be responsible for the large value derived for β . For the parent probe DPH in multilayer systems it has been found that β increases with bilayer water content (Van Ginkel et al., 1986; Van Langen et al., 1987).

Effect of imposed electrical potentials

The effect of applying an external potential to the ITO film on the ordering in the various DPPC/DPH₂PC layers was

investigated in the range from +800 mV to -150 mV (versus Ag/AgCl/saturated KCl) in 0.1 M KNO₃. Under these conditions virtually no electrochemical reactions take place at the ITO surface. Below -150 mV hydrogen evolution becomes significant. During the TIRF measurements as a function of applied potential, the total fluorescence intensity remained practically constant, indicating that the phospholipid layers stay stable on the surface. Imposing a potential on the interface never resulted in a significant change in the derived values for the angle β between absorption and emission dipole moments.

It was found that with decreasing potential the $(\langle P_2 \rangle, \langle P_4 \rangle)$ combinations for phospholipid monolayers and bilayers on the unmodified ITO surface shift slightly, but systematically toward broader distributions (see Fig. 5, *a* and *b*; $\langle P_2 \rangle = \langle P_4 \rangle = 0$ corresponds to a random distribution). The order parameters returned to their original values when the potential application was interrupted, which shows that the changes in ordering are reversible. In fact, we did not expect here to see large effects of imposed potentials: polarization of the substrate surface will only increase the affinity of the lipid headgroups for the surface in comparison to that of the tails, and the headgroups are already at the ITO surface before a potential is imposed. The small shift toward more random ordering is probably the result of the onset of hydrogen evolution as the potential becomes more negative.

For the monolayer on hydrophobized ITO the effect of applying a potential is considerably larger and shows an opposite trend: now the shift in the order parameters increases when the potential becomes more positive (Fig. 5 *c*). In this case the changes in ordering are not completely reversible; when returning to the open circuit potential, the order parameters do not return all the way to their original values. At an imposed potential of +800 mV the derived $(\langle P_2 \rangle, \langle P_4 \rangle)$ combinations correspond to an orientation distribution in which nearly all of the DPH₂PC probes are oriented more or less parallel to the substrate surface (Fig. 6). This may be explained from a competition between headgroups and hydrocarbon tails for access to the interface as the surface becomes more polarized. According to theoretical calculations of Leermakers and Nelson (1990), similar phenomena are the cause for changes in the capacitance of phospholipid monolayers on the mercury/aqueous solution interface. As in our study, on mercury the lipid tails are initially directed toward the substrate surface. However, in comparison to the theoretical and experimental findings for the mercury system, on the hydrophobized ITO surface the changes in orientation are much more gradual and are not completely reversible.

The electrochemistry of Fe(CN)₆^{4-/3-} and Ru(bipyridyl)₃^{2+/3+} at ITO: influence of the presence of DPPC monolayers and bilayers

We investigated the effect of the presence of the phospholipid layers on the reduction and oxidation of Fe(CN)₆^{4-/3-}

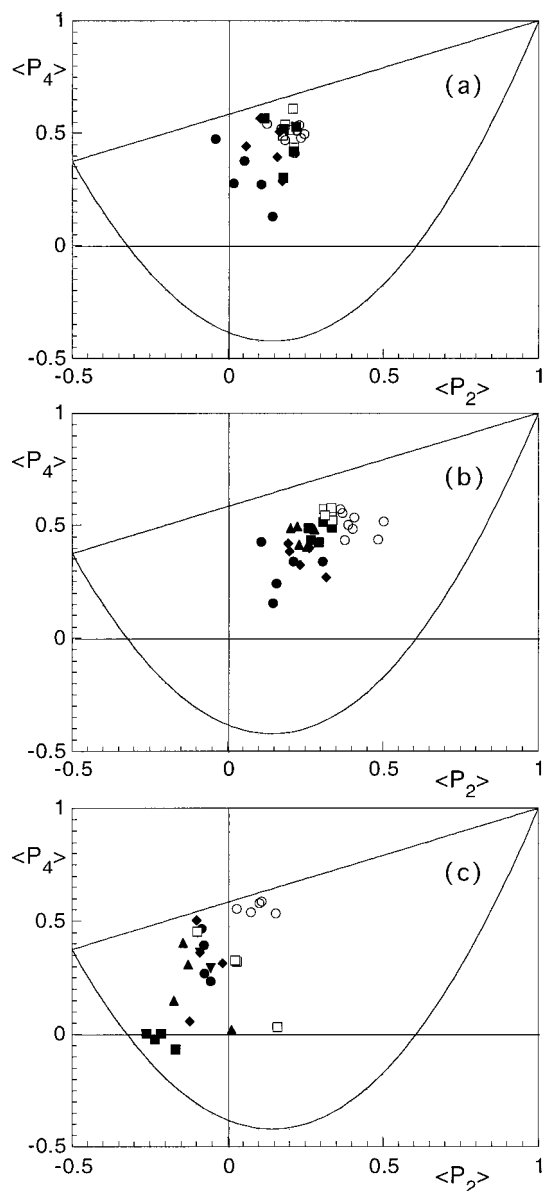


FIGURE 5 Effect of the applied potential on the order parameters of DPPC/DPHPC layers on ITO. (a) Monolayers on a hydrophilic surface. (b) Bilayers on a hydrophilic surface. (c) Monolayers on a hydrophobic surface (ITO-CH₃). ○, Equilibrium potential (open circuit); ■, +800 mV versus Ag/AgCl/saturated KCl. ▲, +400 mV. ◆, 0 mV. ●, -150 mV. □, Order parameters after returning to the open circuit potential.

and Ru(bipyridyl)₃^{2+/3+} at the ITO surface. These redox couples show clear oxidation and reduction peaks at the bare, unmodified ITO surface, as can be seen in Figs. 7 and 8. The positions of the peaks as obtained at a scan rate of 1 mV/s do not shift when the scan rate is further decreased. For Fe(CN)₆^{4-/3-} the reactions are nearly reversible, the distance between the peaks amounting to ~65 mV. (For a fully reversible one-electron transfer process, a separation between cathodic and anodic peaks of 57 mV at 20°C is predicted (Bard and Faulkner, 1980).) For Ru(bipyridyl)₃^{2+/3+} the reactions are less reversible. For this redox couple the distance between the peaks is ~100 mV.

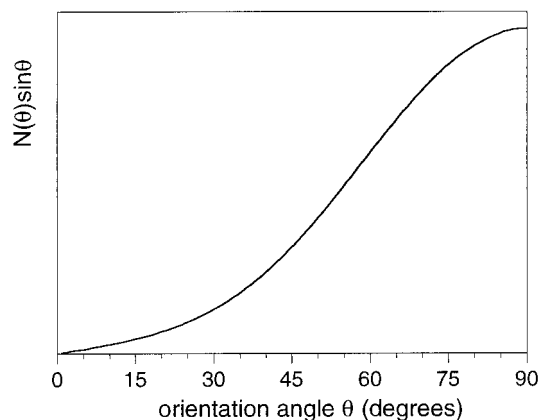


FIGURE 6 Orientation distribution (number density function) calculated from the average (overall) order parameters obtained for DPPC/DPHPC monolayers on hydrophobized ITO at an imposed interfacial potential of +800 mV versus Ag/AgCl/saturated KCl.

The presence of DPPC monolayers or bilayers on unmodified ITO does not have a dramatic effect on the electrochemistry of both redox couples: the peak currents in the voltammograms decrease, respectively, by ~10% and ~20% with respect to bare ITO (Figs. 7 and 8). Furthermore, the distance between the anodic and cathodic peaks becomes somewhat larger, indicating that the electrochem-

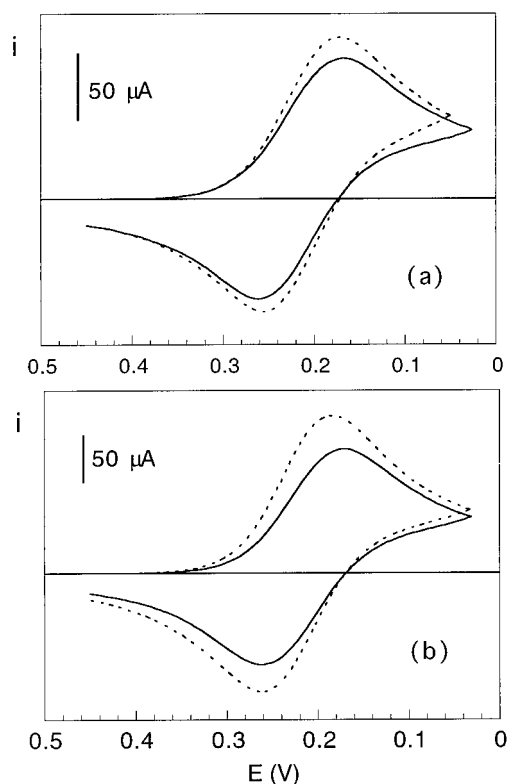


FIGURE 7 Cyclic voltammograms of an ITO/quartz electrode in a 1.0×10^{-3} M Fe(CN)₆^{3-/4-}/0.1 M KNO₃ solution. Scan rate: 1 mV/s. —, (a) With a DPPC monolayer at the ITO surface; (b) with a DPPC bilayer. ---, Voltammograms for bare ITO.

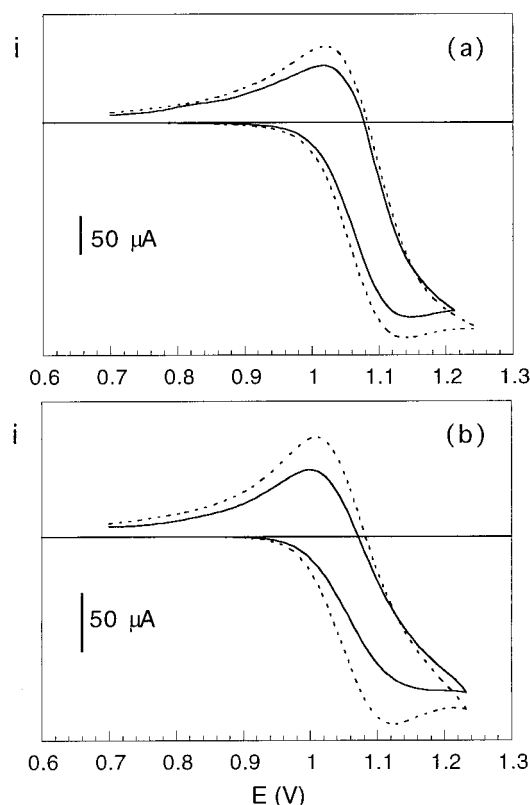


FIGURE 8 Cyclic voltammograms of an ITO/quartz electrode in a 1.0×10^{-3} M $\text{Ru}(\text{bipyridyl})_3^{2+}/0.1$ M KNO_3 solution. Scan rate: 1 mV/s. —, (a) With a DPPC monolayer at the ITO surface; (b) with a DPPC bilayer. ---, Voltammograms for bare ITO.

ical reversibility decreases in the presence of a phospholipid layer. This effect is more evident for the bilayers than for the monolayers.

Comparing our results with those of Nelson and van Leeuwen (1989) on the electrochemistry of various metals (Cd, Cu, Eu, Pb, V, and Zn) at a phospholipid monolayer-coated mercury electrode, the differences are remarkable. In the region where the monolayer is assumed to stay stable and compact on the mercury drop, all electrode processes of the metals are inhibited. Reduction of the metal ions always occurred only at the onset of the first peak in the capacitance/potential diagram of the lipid-coated electrode, at potentials much more negative than for their reduction at the bare electrode. This capacitance peak has been explained as resulting from reorientation of the phospholipid molecules in the monolayer (Leermakers and Nelson, 1990; Nelson and Leermakers, 1990).

At first instance, presuming that the levels of structural organization of the lipids on ITO and mercury are comparable, we expected to see similar effects for the DPPC layers on ITO, i.e., inhibition of electrode processes as long as the phospholipid layers stay rather undisturbed on the ITO surface. $\text{Fe}(\text{CN})_6^{4-/3-}$ and $\text{Ru}(\text{bipyridyl})_3^{2+/3+}$ are very stable and relatively large metal complexes, and it is apparent that they cannot pass through the lipid layers. However, in

contrast to the redox species of the metals investigated at the lipid-coated mercury electrode, in our experiments both redox species are in solution. This implies that only charge transfer across the lipid layers is sufficient to get an electrochemical response. The metal ions used in the experiments of Nelson et al. pass the lipid monolayer, because the reduced species (metal) dissolves in the mercury. For very thin organic films, sufficiently free from pinhole defects, where redox species are effectively blocked from the electrode surface, charge transfer can occur by electron tunneling (Miller et al., 1991). The rate of tunneling decreases exponentially with the thickness of the insulating film. In our case, however, only a linear decrease in the peak currents is observed in going from a monolayer to a bilayer. Apparently, electron tunneling is not the dominant mechanism. Charge transfer probably occurs through small defects in the lipid layers, where the ITO surface is accessible for water and small ions. Spatial fluctuations in ordering have been reported to significantly enhance the permeability of lipid bilayers for small polar molecules (Clerc and Thompson, 1995). Because the mercury/solution interface is perfectly smooth, it is expected that lipid layers at this interface are more compact and have fewer and smaller defects than at a solid substrate like ITO. It would be interesting to see whether the electrode processes of redox couples like $\text{Fe}(\text{CN})_6^{4-/3-}$ and $\text{Ru}(\text{bipyridyl})_3^{2+/3+}$ at mercury are blocked by a lipid monolayer.

For the hydrophobized ITO surface only the redox reactions of the $\text{Ru}(\text{bipyridyl})_3^{2+/3+}$ couple were investigated. The current peaks in the voltammogram (Fig. 9) are much lower, and the electrochemistry is much more irreversible in comparison with the results for the unmodified ITO surface. Now the presence of a phospholipid monolayer facilitates the oxidation and reduction of $\text{Ru}(\text{bipyridyl})_3^{2+/3+}$: the anodic and cathodic peaks are clearer and larger, and the distance between the peaks is somewhat smaller when a DPPC monolayer is present at the hydrophobized surface.

It is remarkable that hydrophobization of the ITO surface with dichlorodimethylsilane has a much larger impact on

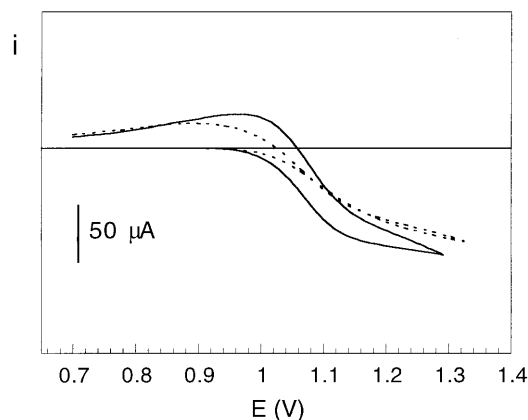


FIGURE 9 As in Fig. 8, for a hydrophobized ITO/quartz electrode with (—) and without (---) a DPPC monolayer.

the electrochemistry of $\text{Ru}(\text{bipyridyl})_3^{2+/3+}$ than the presence of a lipid monolayer or bilayer. Maybe it is difficult for the redox species to approach the hydrophobic surface and adequately interact with it. By deposition of an LB monolayer on the hydrophobized ITO surface, the surface becomes hydrophilic again, and this promotes the electron transfer reaction, although not to a large extent. Also in the case of a DPPC monolayer on unmodified ITO, the resulting surface is hydrophobic, but this only gives a small reduction in the current peaks (Fig. 7 a). Apparently, the surface CH_3 layer is more compact than the DPPC monolayer and blocks the electron transfer more effectively.

CONCLUSIONS

We have investigated the order in DPPC monolayers and bilayers on unmodified (hydrophilic) ITO surfaces and in DPPC monolayers on hydrophobized ITO. At the equilibrium potential of the interface, for all lipid layers combinations of order parameters ($\langle P_2 \rangle$, $\langle P_4 \rangle$) were derived that correspond to bimodal orientation distributions, as calculated by the maximum-entropy method. This suggests that only part of the probe is aligned with the DPPC molecules and reflects the order in the lipid layers, whereas the rest of the probe molecule is lying more or less flat on the substrate surface. This is different from the situation for similar monolayers on quartz, for which orientation distributions with only one maximum were obtained. A cause for this difference may be strong specific interactions between the ITO surface and the DPH-containing tail of the probe. It should be stressed, however, that interactions between DPH and the substrate surface may result in violations of the cylindrical symmetry and probe geometry assumptions made in the theoretical model underlying the analysis of the fluorescence data. Furthermore, fast rotational movements of the DPH-containing tail of the probe lipid are neglected in the model. Although this seems to be a reasonable assumption for the systems studied here, there still may be some "dynamic" contribution to the derived order parameters and the angle between the absorption and emission dipole moment of the DPH moiety. If, indeed, a significant part of the DPH₂PC molecules is flat on the substrate surface, this may imply that the probe is less suitable for studying structural features of such layers on ITO. Therefore, we also plan to investigate the effect of imposed potentials for phospholipid layers on gold films.

For DPPC monolayers and bilayers on the unmodified ITO surface, the effect of applying potentials to the substrate is small. This is in line with what was expected, because for these layers the ITO surface is in contact with the polar headgroups. For monolayers on hydrophobized ITO, where the lipid tails are initially directed toward the surface, the derived combinations of order parameters shift in such a way that more probes are parallel to the surface as the potential increases. This is in line with what has been found for phospholipid monolayers on a mercury electrode

and can be explained from an enhanced competition between headgroups and tails for access to the surface. Contrary to the observations for lipid-coated mercury electrodes, here the changes in ordering are gradual and are not completely reversible.

Phospholipid Langmuir-Blodgett monolayers and bilayers on a solid substrate like ITO are not sufficient to block redox reactions. Probably because of small defects in the layers, charge transfer between the electrode surface and redox couples in solution is still possible. This is of importance for the application of lipid layers (with built-in functional molecules acting as selectors for the detection of specific compounds) in electrochemical (bio)sensors.

Mr. Remco Fokink is gratefully acknowledged for technical assistance in improving the TIRF set-up and with the orientation measurements. We are indebted to Dr. Herman P. van Leeuwen for stimulating and valuable discussions.

REFERENCES

- Bard, A. J., and L. R. Faulkner. 1980. *Electrochemical Methods. Fundamentals and Applications*. John Wiley and Sons, New York.
- Bernsdorff, C., R. Winter, T. L. Hazlett, and E. Gratton. 1995. Influence of cholesterol and β -sitosterol on the dynamic behaviour of DPPC as detected by TMA-DPH and PyrPC fluorescence. *Ber. Bunsenges. Phys. Chem.* 99:1479–1488.
- Bevensee, R. M. 1983. *Maximum entropy solutions to scientific problems*. Prentice Hall, Englewood Cliffs, NJ.
- Bos, M. A., and J. M. Kleijn. 1995a. Determination of the orientation distribution of adsorbed fluorophores using TIRF. I. Theory. *Biophys. J.* 68:2566–2572.
- Bos, M. A., and J. M. Kleijn. 1995b. Determination of the orientation distribution of adsorbed fluorophores using TIRF. II. Measurements on porphyrin and cytochrome *c*. *Biophys. J.* 68:2573–2579.
- Bos, M. A., Z. Shervani, A. C. I. Anusiem, M. Giesbers, W. Norde, and J. M. Kleijn. 1994. Influence of the electrical potential of the interface on the adsorption of proteins. *Colloids Surfaces B*. 3:91–100.
- Cheng, K. H. 1989. Fluorescence depolarization study of lamellar liquid crystalline to inverted cylindrical micellar phase transition of phosphatidylethanolamine. *Biophys. J.* 55:1025–1031.
- Clerc, S. G., and T. E. Thompson. 1995. Permeability of dimyristoyl phosphatidylcholine/dipalmitoyl phosphatidylcholine bilayer membranes with coexisting gel and liquid-crystalline phases. *Biophys. J.* 68:2333–2341.
- Deinum, G., H. van Langen, G. van Ginkel, and Y. K. Levine. 1988. Molecular order and dynamics in planar lipid bilayers: effects of unsaturation and sterols. *Biochemistry*. 27:852–860.
- Florine-Casteel, K. 1990. Phospholipid order in gel- and fluid-phase cell-size liposomes measured by digitized video fluorescence polarization microscopy. *Biophys. J.* 57:1199–1215.
- Gu, D. F., C. Rosenblatt, and Z. Li. 1995. Atomic force microscopy characterization and liquid crystal aligning effect of polymerizable diacetylene Langmuir-Blodgett films. *Liquid Cryst.* 19:489–496.
- Hansen, W. N. 1968. Electric fields produced by the propagation of plane coherent electromagnetic radiation in a stratified medium. *J. Opt. Soc. Am.* 58:380–390.
- Kalb, E., J. Engel, and L. K. Tamm. 1990. Binding of proteins to specific target sites in membranes measured by total internal reflection fluorescence microscopy. *Biochemistry*. 29:1607–1613.
- Kooyman, R. P. H., M. H. Vos, and Y. K. Levine. 1983. Determination of orientational order parameters in oriented lipid membrane systems by angle-resolved fluorescence depolarization experiments. *Chem. Phys.* 81:461–472.

- Leermakers, F. A. M., and A. Nelson. 1990. Substrate-induced structural changes in electrode-adsorbed lipid layers: a self-consistent field theory. *J. Electroanal. Chem.* 278:53–72.
- Lentz, B. R. 1989. Membrane “fluidity” as detected by diphenylhexatriene probes. *Chem. Phys. Lipids.* 50:171–190.
- Mikrut, J. M., P. Dutta, J. B. Ketterson, and R. C. MacDonald. 1993. Atomic-force and fluorescence microscopy of Langmuir-Blodgett monolayers of L- α -dimyristoylphosphatidic acid. *Phys. Rev. B.* 48: 14479–14487.
- Miller, C., P. Cuendet, and M. Grätzel. 1991. Adsorbed ω -hydroxy thiol monolayers on gold electrodes: evidence for electron tunneling to redox species in solution. *J. Phys. Chem.* 95:877–866.
- Mitchell, M. L., and R. A. Dluhy. 1988. In situ FT-IR investigation of phospholipid monolayer phase transitions at the air-water interface. *J. Am. Chem. Soc.* 110:712–718.
- Mulders, F., H. van Langen, G. van Ginkel, and Y. K. Levine. 1986. The static and dynamic behaviour of fluorescent probe molecules in lipid bilayers. *Biochim. Biophys. Acta.* 859:209–218.
- Muller, J. M., E. E. van Faassen, and G. van Ginkel. 1994a. The interpretation of the time-resolved fluorescence anisotropy of diphenylhexatriene-phosphatidylcholine using the compound motion model. *Biochem. Biophys. Res. Commun.* 201:709–715.
- Muller, J. M., E. E. van Faassen, and G. van Ginkel. 1994b. Experimental support for a novel compound motion model for the time-resolved fluorescence anisotropy decay of TMA-DPH in lipid vesicle bilayers. *Chem. Phys.* 185:393–404.
- Muller, J. M., G. van Ginkel, and E. E. van Faassen. 1996. Effect of lipid molecular structure and gramicidin A on the core of lipid vesicle bilayers. A time-resolved fluorescence depolarization study. *Biochemistry.* 35:488–497.
- Nelson, A., and F. A. M. Leermakers. 1990. Substrate-induced structural changes in electrode-adsorbed lipid layers. Experimental evidence from the behaviour of phospholipid layers on the mercury-water interface. *J. Electroanal. Chem.* 278:73–83.
- Nelson, A., and H. P. van Leeuwen. 1989a. Metal voltammetry at dioleoyl lecithin (di-O-PC) coated mercury electrodes: Cd, Cu, Eu, Pb, V and Zn and the effect of electrolyte composition. *J. Electroanal. Chem.* 273: 183–199.
- Nelson, A., and H. P. van Leeuwen. 1989b. Metal voltammetry at dioleoyl lecithin (di-O-PC) coated mercury electrodes: effect of organic complexing agents on Cd voltammetry. *J. Electroanal. Chem.* 273:201–208.
- Parente, R. A., and B. R. Lentz. 1985. Advantages and limitations of 1-palmitoyl-2-((2-(4-(6-phenyl-trans-1,3,5-hexatrienyl)phenyl)ethyl)carbonyl)-3-Sn-phosphatidylcholine as a fluorescent membrane probe. *Biochemistry.* 24:6178–6185.
- Pebay-Peyroula, E., E. J. Dufourc, and A. G. Szabo. 1994. Location of diphenyl-hexatriene and trimethylammonium-diphenyl-hexatriene in dipalmitoylphosphatidylcholine bilayers by neutron diffraction. *Biophys. Chem.* 53:45–56.
- Safinya, C. R. 1997. Biomolecular materials: structure, interactions and higher order self-assembly. *Colloids Surfaces A.* 128:183–195.
- Salamon, Z., Y. Wang, G. Tollin, and H. A. Macleod. 1994. Assembly and molecular organization of self-assembled lipid bilayers on solid substrates monitored by surface plasmon resonance spectroscopy. *Biochim. Biophys. Acta.* 1195:267–275.
- Siontorou, C. G., D. P. Nikolelis, U. J. Krull, and K. L. Chiang. 1997. A triazine herbicide minisensor based on surface-stabilized bilayer lipid membranes. *Anal. Chem.* 15:3109–3114.
- Tamm, L. K., and H. M. McConnell. 1985. Supported phospholipid bilayers. *Biophys. J.* 47:105–113.
- Tien, H. T., Z. Salamon, W. Liu, and A. Ottova. 1993. Immobilization of ferrocene on a BLM system—an amperometric sensor of $\text{Fe}(\text{CN})_6^{3/-4}$ ions. *Anal. Lett.* 26:819–829.
- Van Ginkel, G., L. J. Korstanje, H. van Langen, and Y. K. Levine. 1986. The correlation between molecular orientational order and reorientational dynamics of probe molecules in lipid multibilayers. *Faraday Discuss. Chem. Soc.* 81:49–61.
- Van Langen, H., D. Engelen, G. van Ginkel, and Y. K. Levine. 1987. Headgroup hydration in egg-lecithin multibilayers affects the behaviour of DPH probes. *Chem. Phys. Lett.* 138:99–104.
- Zhai, X., and J. M. Kleijn. 1997a. Order in phospholipid Langmuir-Blodgett monolayers determined by total internal reflection fluorescence. *Biophys. J.* 72:2651–2659.
- Zhai, X., and J. M. Kleijn. 1997b. Molecular structure of dipalmitoylphosphatidylcholine Langmuir-Blodgett monolayers studied by atomic force microscopy. *Thin Solid Films.* 304:327–332.